Effective Atmospheric Emissivity under Clear Skies

D. O. STALEY
Institute of Atmospheric Physics, The University of Arizona, Tucson
AND G. M. JURICA
Dept. of Geosciences, Purdue University, Lafayette, Ind.

(Manuscript received 24 August 1971)

ABSTRACT

The effective atmospheric emissivity, $F\downarrow/(\sigma T_0^4)$, where $F\downarrow$ is the downward radiative flux density and σT_0^4 the blackbody flux density at the surface temperature T_0, is computed for clear skies and straight temperature and dew-point soundings by means of emissivity integrations. Emissivity data by Jurica and by Staley and Jurica were used, and separate computations made for H_2O, CO_2, H_2O-CO_2 overlap, and O_3. The effective atmospheric emissivity depends almost entirely on surface vapor pressure, decreases slightly with increasing surface elevation, and is essentially independent of surface temperature. The contribution by CO_2 decreases from about 0.19 to about 0.17 as surface elevation increases from sea level to 710 mb. The contribution of overlap is negative and increases rapidly with increasing surface vapor pressure, becoming comparable to the CO_2 contribution for very large vapor pressures. Measurements support the computations, but suggest, as has been found before, additional downward flux density from aerosols or from as yet unspecified trace gases.

1. Introduction

The purpose of this paper is twofold: 1) to evaluate the relative contributions of H_2O, CO_2, H_2O-CO_2 overlap, and O_3 to the downward radiative flux density at the earth's surface for simple sounding types utilizing emissivity data presented by Staley and Jurica (1970) and by Jurica (1970); and 2) to take note of the relationship of effective atmospheric emissivity to surface moisture in the special but important case of soundings with straight temperature and dew-point profiles on a Stüve diagram.

The relative contributions to the flux density are of interest because the emissivities used differ from and presumably improve upon previous emissivities, and because the definition and magnitude of the overlap correction differ from those of Elsasser and of Zdunkowski *et al.* (1966). Historically there has been considerable interest in empirical relationships for the effective atmospheric emissivity; Swinbank (1963) notes that although the present day availability of radiometers obviates the reliance on empirical expressions, estimates of downward flux density from climatological data are sometimes necessary, and estimates over oceans must largely rely on surface observations.

2. Effective atmospheric emissivity

The downward flux density from clear skies is most conveniently interpreted in terms of the dimensionless ratio, $F\downarrow/(\sigma T_0^4)\equiv\epsilon_a$, where σ is the Stefan-Boltzmann constant, T_0 the temperature at the lower boundary of the atmosphere, and ϵ_a an "effective atmospheric emissivity" based on the temperature at the lower boundary of the atmosphere. At night the downward flux density itself is composed of the partial flux densities of H_2O, CO_2, O_3, aerosol, and other trace gas emitters, in order of probable decreasing importance. The flux density of aerosol can conceivably exceed that of O_3 under some conditions. The possible importance of aerosol radiation has been noted by Robinson (1966). It is certainly a highly variable and poorly understood contribution. Other trace gas emitters cannot be ruled out entirely so long as the downward flux density is not entirely accounted for (Robinson, 1950). Some aspects of the role of trace gases on infrared absorption have been discussed by Kozyrev and Bazhenov (1969).

For purposes of computation, it is convenient to express the total downward flux density $F\downarrow$ as

$$F\downarrow=F\downarrow(H_2O)+F\downarrow(CO_2)+F\downarrow(H_2O\text{-}CO_2\text{ overlap})+F\downarrow(O_3)+F\downarrow_d+F\downarrow_g, \quad (1)$$

where the first two terms on the right represent the flux densities contributed, respectively, by H_2O and CO_2, each in the absence of the other. The third term represents the flux density contribution (negative) associated with overlap of H_2O and CO_2 bands. The fourth term represents the flux density contribution of ozone, assumed not to overlap the emission of the other

gases. The fifth term represents the flux density contribution of aerosols plus any overlap effect between aerosols and the emitting gases. The final term represents the contribution of any other trace gas emitters. If the individual flux density contributions in the first four terms of Eq. (1) are expressed in terms of integrations of blackbody flux density over emissivity, the effective atmospheric emissivity becomes

$$\epsilon_a=\frac{F\downarrow}{\sigma T_0^4}=\frac{\overbrace{\int_0\sigma T^4 d\epsilon}^{\epsilon_T(H_2O)}}{\sigma T_0^4}+\frac{\overbrace{\int_0\sigma T^4 d\epsilon}^{\epsilon_T(CO_2)}}{\sigma T_0^4}+\frac{\overbrace{\int_0\sigma T^4 d\epsilon}^{[(\Delta\epsilon)_T(\text{overlap})]}}{\sigma T_0^4}+\frac{\overbrace{\int_0\sigma T^4 d\epsilon}^{\epsilon_T(O_3)}}{\sigma T_0^4}+\frac{F\downarrow_d}{\sigma T_0^4}+\frac{F\downarrow_g}{\sigma T_0^4}, \quad (2)$$

$$=\overbrace{\int_0\left(\frac{T}{T_0}\right)^4 d\epsilon}^{\epsilon_T(H_2O)}+\overbrace{\int_0\left(\frac{T}{T_0}\right)^4 d\epsilon}^{\epsilon_T(CO_2)}+\overbrace{\int_0\left(\frac{T}{T_0}\right)^4 d\epsilon}^{[(\Delta\epsilon)_T(\text{overlap})]}+\overbrace{\int_0\left(\frac{T}{T_0}\right)^4 d\epsilon}^{\epsilon_T(O_3)}+\frac{F\downarrow_d}{\sigma T_0^4}+\frac{F\downarrow_g}{\sigma T_0^4},$$

$$=\epsilon_a(H_2O)+\epsilon_a(CO_2)+\epsilon_a(\text{overlap})+\epsilon_a(O_3)+\epsilon_a(\text{aerosols})+\epsilon_a(\text{trace gases}),$$

where the upper limits denote the values of the indicated flux emissivities corresponding to the top of the atmosphere.

3. Computations for H_2O

Rodgers (1967) has discussed the errors introduced by applying emissivities for homogeneous slabs to computations of atmospheric flux densities. Errors in the downward flux density computation were smallest in the lower troposphere, a not too surprising result in view of the fact that most of the water vapor is to be found in the lower troposphere and the bulk of downward flux density is contributed by layers near the surface having temperatures and pressures not very different from surface values.

The errors introduced by computation from laboratory emissivity data depend on the accuracy of the data for standard conditions and the method of taking into account the heterogeneity of the atmospheric slab. Preliminary computations were made utilizing emissivities determined by Staley and Jurica (1970) on the basis of Elsasser and Culbertson's (1960) transmissivity data. Linear pressure scaling of optical depth was used, but it has the effect of unrealistically reducing optical depth. The actual pressure dependence for overlapping lines as determined from data of Wyatt *et al.* (1962) and others, is less than linear. Jurica (1970) has shown that values of n such that $\epsilon[u,p,T]=\epsilon[u(p/p_0)^n,p_0,T]$, where u is optical depth, p pressure, $p_0=1$ atm, and T temperature, depend on temperature, pressure, and, especially, optical depth. Values of n range from about 0.7 for small optical depths to about 1.0 for large optical depths. Furthermore, scaling according to the pressure at the level of integration excessively reduces the optical depth. These factors lead to an underestimate of the downward flux density.

The preferred computations for H_2O given here were based on pressure- and temperature-dependent emissivities determined by Jurica from the laboratory transmissivity data presented by Wyatt *et al.* and others. These transmissivities were based on finer spectral resolution, and pressure and temperature dependences were more accurately evaluated, than in the case of the transmissivities of Elsasser and Culbertson. A property of the Jurica emissivities is that they are of the order of 0.02 larger, for typical total atmospheric optical depths, than the emissivities based on the Elsasser and Culbertson data. Furthermore, they are a function of pressure, and computations can be made taking into account the actual mean pressure below the level of integration. As a consequence, larger downward flux densities for water vapor are obtained by using the Jurica emissivities. This is a desirable feature in view of the still unexplained findings of Robinson (1950) that the measured atmospheric downward flux density exceeds the computed flux density. This is not to say, however, that the discrepancy has been resolved, or even that it traces to a hitherto underestimated H_2O flux density. Measurements much more accurate than the few examples presented in this paper would be necessary to resolve the matter. It is possible that significant radiation is contributed by aerosol and/or unspecified trace gases, neither of which is included in the computations.

The integrations for H_2O, CO_2 and H_2O-CO_2 overlap were carried out according to

$$F\downarrow=\sum_{n=1}^{N}\overline{\sigma T_n^4}\Delta\epsilon_n, \quad (3)$$

where N is the number of atmospheric layers above the reference level and the bar denotes an average over a layer. In the case of H_2O, the Curtis-Godson effective pressure

$$p_e=\frac{1}{u_t}\int_0^{u_t}p\,du \quad (4)$$

was evaluated for each optical depth u_t, and positive increments of emissivity were obtained from curves of emissivity vs optical depth at the appropriate p_e for the level of integration. The variation of emissivity

with temperature over the range of temperatures found in the lower troposphere, from which the bulk of the flux density is contributed, is negligibly small; hence, emissivities for slabs at surface temperatures were used.

4. Computations for CO_2

For the CO_2 integration the emissivities used were determined by Staley and Jurica (1970) from Elsasser and Culbertson's (1960) generalized absorption coefficients and flux transmissivities. Layers of 1-mb thickness were used immediately above the reference level, and gradually increased as the distance from the reference level increased. The use of emissivities for isothermal slabs is particularly justified in the case of the downward flux density from CO_2 in the lower troposphere, since 1) most of the flux density arriving at the reference level is contributed by layers extremely close to the reference level having temperatures and pressures almost the same as that of the reference level, and 2) the dependence of CO_2 slab emissivities on temperature is very small. The emissivities of isothermal slabs having an optical depth of 1 cm are 0.0826 and 0.0823 for −10C and 20C, respectively. For 10 cm the corresponding emissivities are 0.139 and 0.141, while for 100 cm the emissivities are 0.193 and 0.196. Since emissivities corresponding to temperatures at the reference level were used, and temperature varies by much less than the above temperature difference over a layer from which the bulk of the CO_2 flux density is contributed, the error introduced by using isothermal emissivities is small indeed. In the absence of emissivity data for pressure other than standard, linear pressure scaling of optical depth was used, although the accuracy of this type of scaling is difficult to assess. If the actual variation of emissivity with pressure is known, the error introduced by linear pressure scaling may be determined. Both theoretical and experimental evidence led Elsasser to conclude that the pressure-dependence of absorption in the 15 μ CO_2 band should be represented by a $p^{0.88}$ pressure correction to optical depths. Thus, a linear pressure correction would underestimate optical depth and, hence, would result in an underestimation of downward flux density. In order to allow the consistent application of a linear factor to his data, Elsasser adjusted his generalized absorption coefficient values so that results equivalent to those obtained using a $p^{0.88}$ correction would result from the use of a linear correction factor. The errors associated with pressure scaling should be smallest when the reference level pressure is near standard, largest when the reference level pressure is substantially less than standard. In the lower troposphere, flux density errors associated with pressure scaling probably are no worse than those that arise from different but equally justifiable treatments of the basic absorption data which lead to different emissivities for standard pressure.

The emissivity $F\downarrow(CO_2)/(\sigma T^4)$ was calculated as a function of pressure and constant CO_2 mixing ratio in an atmosphere having the temperatures of the standard atmosphere at sea level and the tropopause, with the tropospheric temperature distribution given by a straight line on a Stüve diagram, and the stratosphere isothermal. It is unnecessary to make computations for colder or warmer soundings, since $F\downarrow(CO_2)$ is almost exactly proportional to σT^4, and the ratio $F\downarrow(CO_2)/(\sigma T^4)$ is essentially insensitive to reference level temperature at a given pressure level. However, the presence of a strong temperature inversion would increase the emissivity very slightly. The mixing ratios assumed here were 2, 5, and 8×10^{-4} gm gm^{-1}, the intermediate value being the mean observed mixing ratio, while the other values lie well within extremes observed near the earth's surface.

The downward radiative flux density from CO_2 has often been expressed by

$$F\downarrow(CO_2)=b\sigma T^4, \tag{5}$$

where b is a constant and T is the temperature at the reference level.

The expression of the CO_2 flux density by (5) traces to Elsasser (1942) and is based on the argument that CO_2 absorbs so strongly in the dominant 15 μ CO_2 band that a thin atmospheric layer is a blackbody in this range. It was recognized that such a formulation could not apply to the higher atmosphere where appreciable temperature change can occur over a small optical depth. Elsasser indicated a value of the order of 0.18 for b. The most frequently quoted (e.g., Haltiner and Martin, 1957) value of b is 0.185, which is apparently due to Robinson (1947). These values appear to be based on the percentage of total blackbody radiation contained within a somewhat subjectively chosen wavelength interval, rather than on calculations of $F\downarrow(CO_2)$.

Kondrat'yev (1965) has argued that 0.185 is unrealistic since to obtain this value the remote parts of the band wings must be included, and absorption cannot be expected to be complete in the far wings. It is therefore clear that, even in the troposphere, where most of the CO_2 flux density may be contributed by nearby layers, some will be contributed by more distant layers having different temperatures. The influence of distant layers must depend on the CO_2 concentration and the rate of change of temperature with CO_2 optical depth. Hence, we anticipate that no universally constant value of b can be obtained. Only computations can determine its magnitude and variability.

Fig. 1 shows the results for CO_2. The quantity b is seen to be a variable coefficient which decreases with height and increases with mixing ratio. The decrease with height traces physically to the decrease of total optical depth, and, to a lesser extent, to a slight decrease in emissivity with decrease of temperature. The range of mixing ratio assumed is probably unreal-

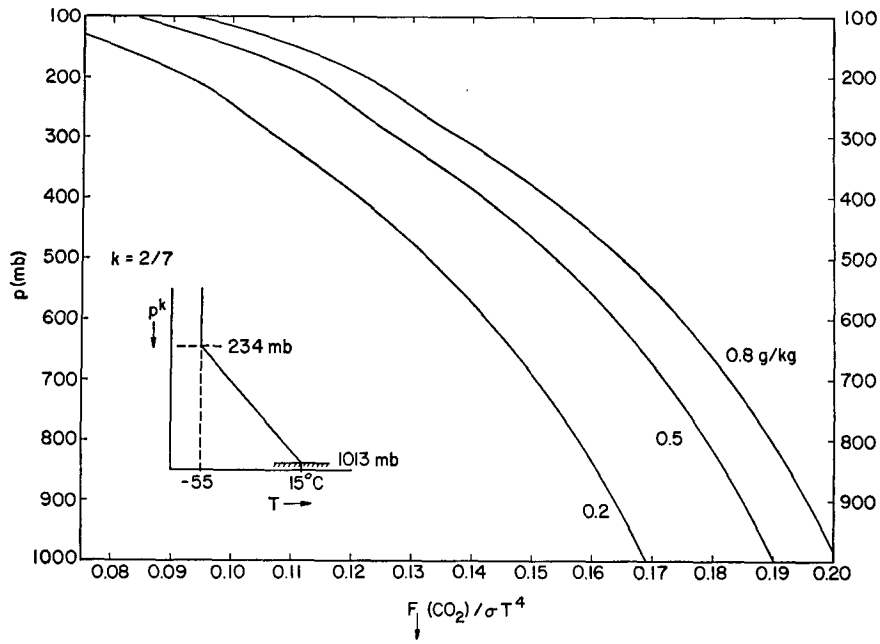

FIG. 1. The effective atmospheric emissivity of CO_2, $F\downarrow(CO_2)/(\sigma T^4)$, as a function of reference level pressure p_0 and mixing ratio for a straight temperature sounding as depicted in the inset diagram.

istically large above levels influenced directly by vegetation. However, if the CO_2 flux density originates almost entirely from air layers a very short distance above the reference level, then the values of b corresponding to the extreme mixing ratios would, on occasion, be realistic, depending on time of day and presence or absence of surface vegetation. Fig. 1 allows some improvement over $b=0.185$, especially at pressures <800 mb.

To assess the extent to which CO_2 radiation originates in layers near the reference level, the percentage of the total flux density arriving at the reference level was calculated as a function of pressure above the reference level. The results, assuming a constant 5×10^{-4} gm gm^{-1} mixing ratio, are shown in Fig. 2 for the reference level at 1000 and 500 mb. More than 75% of the CO_2 flux density is contributed from the first 50 mb above the reference level.

In the computations which follow, the contribution $\epsilon_a(CO_2)$ to the effective atmospheric emissivity ϵ_a was based on the mean mixing ratio, 5×10^{-4} gm gm^{-1}. Accordingly, $\epsilon_a(CO_2)=0.191$, 0.182 and 0.173 at 1013, 840 and 710 mb, respectively, the levels for which calculations of ϵ_a were made for a variety of H_2O distributions.

5. Computations for overlap

The contribution of H_2O-CO_2 overlap to the effective atmospheric emissivity is negative. It was calculated by means of the overlap emissivity correction tables given by Staley and Jurica (1970). [For greater consistency, the overlap emissivity correction should be based on the data used by Jurica (1970) to obtain the H_2O emissivities; however, the overlap correction is only the third largest term in (2), and the small error is tolerable.] The CO_2 mixing ratio was again assumed to be 5×10^{-4} gm gm^{-1} throughout. Selection of a vertical H_2O distribution then implies a relationship

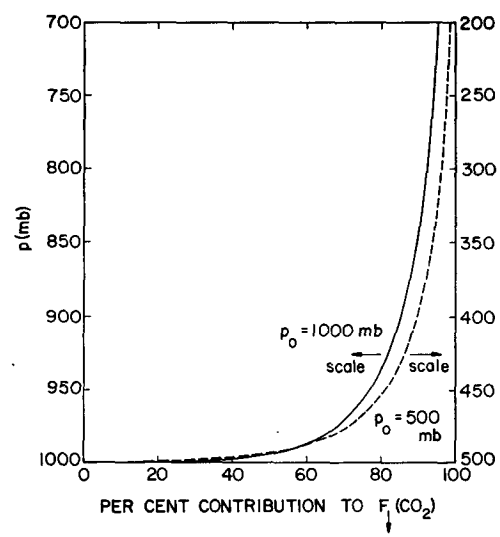

FIG. 2. The cumulative contribution to the downward CO_2 flux density at the reference level p_0 as a function of pressure above the reference level. The abscissa gives the percentage of the total downward flux density contributed by layers between the corresponding pressure p and the reference level p_0 (1000 or 500 mb). The CO_2 mixing ratio is 0.5 gm kg^{-1}, while the sounding is shown in Fig. 1.

between H_2O and CO_2 optical depths. The overlap correction is a function of H_2O and CO_2 optical depths. Hence, the sounding may be represented as a path through a field of overlap corrections plotted on a graph of H_2O vs CO_2 optical depths. Essentially this is a path through the overlap correction tables given by Staley and Jurica. By relating sounding temperature to optical depths, the third integral on the right-hand side of Eq. (2) can be evaluated. (Linear scaling of optical depth was used, but the overlap correction is small, and near the surface the scaling is not crucial.) The overlap emissivity correction is based on an isothermal column, and the tables show that the dependence on the temperature of the column cannot be neglected. Computations show that most of the overlap correction is contributed by air layers near the reference level. Therefore, the overlap integral in Eq. (2) was calculated by means of the overlap tables for the two nearest temperatures, one above and one below the surface temperature, and the final overlap correction arrived at by interpolation.

Fig. 3 shows the contribution of overlap correction as a function of surface vapor pressure for three surface pressures and soundings depicted by the inset diagram. Temperatures at 1013 mb and the tropopause are those of the standard atmosphere, but are connected with straight lines. Computations were carried out for four vapor pressures at each pressure, and connected by smooth curves. The correction increases rapidly with increasing vapor pressure at small vapor pressures, but more gradually at the larger vapor pressures. For $e=15$ mb and $p=1013$ mb, the overlap correction is more than 50% of the CO_2 contribution. For very large vapor pressures the overlap correction becomes comparable to the CO_2 contribution.

6. Ozone computation

The contribution of O_3 to the effective atmospheric emissivity was based on the assumption of 0.30 cm total O_3, a value appropriate to June or July at 30–35N.

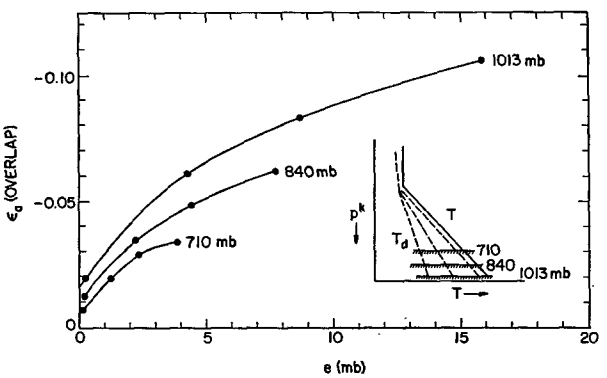

FIG. 3. The H_2O-CO_2 overlap contribution for soundings depicted schematically in the inset diagram. Calculations were made at the four points on each curve.

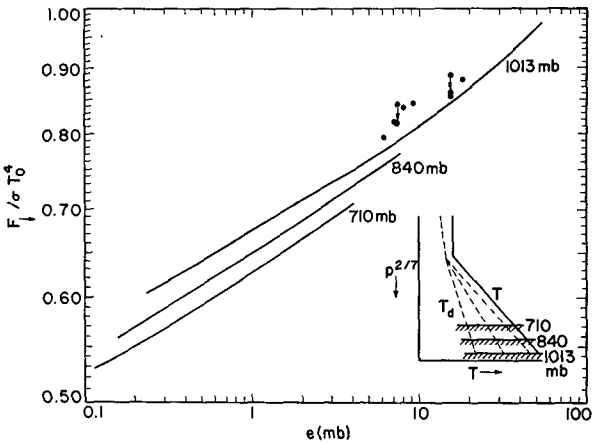

FIG. 4. The effective atmospheric emissivity, $\epsilon_a=F\downarrow/(\sigma T_0^4)$, as a function of surface vapor pressure and surface elevation for straight temperature and dew-point soundings as depicted schematically in the inset diagram. Points represent ϵ_a determined from net radiation measurements by Sellers and Dryden (1967).

The corresponding isothermal emissivities, taken from the tables by Staley and Jurica, are 0.068, 0.057 and 0.043 for 20, −10 and −40C, respectively. (Emissivities for 0.45 cm total O_3 are of the order of 0.01 larger.) Several O_3 soundings shown by Junge (1963) indicate that the troposphere contains on the order of 0.025 cm of O_3. Although this is less than a tenth of the total atmospheric O_3, the corresponding isothermal emissivities are more than half the values noted above for 0.30 cm total O_3. Because of the great variability of emissivity with temperature, the computation of the O_3 flux density is subject to large percentage errors. Fortunately, the total contribution of O_3 is small, so that errors are not crucial to the present investigation. In view of the several uncertainties and the $(T/T_0)^4$ weighting factor, which in this case should be somewhat less than unity, the contribution of O_3 to the effective atmospheric emissivity was assumed throughout to be 0.05. This value may readily be in error by ± 0.01, and possibly by as much as ± 0.02. It is of interest to note that the O_3 contribution tends to cancel the overlap contribution, although the latter is rather dependent on vapor pressure.

7. Results

All computations of the effective atmospheric emissivity were based on the simplest sounding type of interest, one in which temperature and dew-point distributions can be represented as straight lines on a Stüve diagram. It soon became apparent, as noted above for CO_2, that shifts (toward higher or lower temperatures) of the straight line temperature distribution had an almost imperceptible effect on the effective atmospheric emissivity, the reason being that the $(T/T_0)^4$ weighting factor in (2) is nearly independent of T_0. Hence, a single temperature curve sufficed for

TABLE 1. Computed effective atmospheric emissivity ϵ_a at 1013 mb as a function of surface vapor pressure for straight temperature and dew-point soundings. See text for explanation of J and S, J.

e (mb)	H_2O J	H_2O (S, J)	CO_2	Overlap	O_3	Total
0.237	0.38	(0.35)	0.19	−0.02	0.05	0.60
0.706	0.44	(0.41)	0.19	−0.03	0.05	0.65
1.83	0.51	(0.47)	0.19	−0.04	0.05	0.71
4.22	0.57	(0.53)	0.19	−0.06	0.05	0.75
6.14	0.60	(0.56)	0.19	−0.07	0.05	0.77
8.73	0.65	(0.59)	0.19	−0.09	0.05	0.80
15.8	0.71	(0.65)	0.19	−0.11	0.05	0.84
31.9	0.82		0.19	−0.14	0.05	0.92
51.7	0.89		0.19	−0.17	0.05	0.96

all dew-point distributions short of supersaturation. Surface dew-point depressions were varied from 0 to 40C and connected by straight lines to a dew-point depression of 1C at the tropopause. For the higher dew points, the 1013-mb temperature was assumed to be 40C, and the tropopause at 90 mb with a temperature of −62C. This required some extrapolation of the overlap tables, the highest of which is for 20C, but the increase of the correction with temperature is very small at higher temperatures. In any event, observed temperatures for a given surface dew point are variable, necessitating a small uncertainty.

The total effective atmospheric emissivity resulting from H_2O, CO_2 H_2O-CO_2 overlap, and O_3 is depicted as a function of surface vapor pressure and surface total pressure in Fig. 4. (For dew-point temperatures at and below −40C, vapor pressures were computed with respect to an ice surface; at and above OC, vapor pressures were computed with respect to a flat, liquid water surface. Between these two dew-point temperatures, vapor pressures were computed utilizing a latent heat varying linearly with temperature between its value at −40 and 0C.) The individual contributions to the effective atmospheric emissivity are shown in Table 1, where J denotes H_2O computations by means of Jurica's emissivities and effective homogeneous pressures, while (S,J) denotes computations by means of emissivities given by Staley and Jurica using linear pressure scaling of optical depth.

Except at the highest vapor pressures at 1013 mb, the nearly straight curves in Fig. 4 indicate that ϵ_a is approximately proportional to a power of vapor pressure. The more rapid increase of ϵ_a with e at high values of e at 1013 mb traces to the increased emission in the atmospheric window, which introduces a rapid increase of water vapor emissivity with optical depth for large optical depth (Staley and Jurica, 1970).

The effect on ϵ_a of surface elevation is fairly small, but is roughly constant at all vapor pressures; ϵ_a decreases by about 0.05 from 1013 to 710 mb over the range of vapor pressures shown in the diagram, and by only about 0.02 from 1013 to 840 mb. Such a small effect could easily be masked by other effects, such as departure of the moisture profile from that of a straight line on the Stüve diagram. The small decrease of ϵ_a with elevation is physically related to the slight decrease of total optical depth with elevation for the condition of constant vapor pressure. This was verified by computations of the total optical depth in the three cases, and occurs despite the fact that surface mixing ratio increases upward when vapor pressure is held constant.

The curve for 1013 mb in Fig. 4 can be represented reasonably well, for the range $0.2 \leqslant e \leqslant 20$ mb, by

$$\epsilon_a = \frac{F\downarrow}{\sigma T_0^4} = Ce^m, \tag{6}$$

where $C=0.67$ and $m=0.080$. The curve for 710 mb can be represented reasonably well by using $C=0.63$ and the same m. It must be emphasized that such validity as Eq. (6) may have is limited to straight temperature soundings and, especially, straight dew-point soundings on a Stüve diagram. It is not offered as an improvement over the various empirical expressions, such as the well-known Brunt formula, for downward longwave flux density under general circumstances. Straight temperature and dew-point soundings are a common occurrence, however, and Eq. (6) may be of value in establishing empirical expressions for ϵ_a applicable to appropriate situations. Systematic computations showed that moisture inversions had a large effect on ϵ_a, while temperature inversions had a very small effect.

Also shown in Fig. 4 are several effective atmospheric emissivities based on measurements by Sellers and Dryden (1967) of net radiation F_n, by means of a Funk (CSIRO) radiometer over desert soil at Tucson, Ariz., on several nights in the summer of 1965. In order to recover the effective emissivity $[\epsilon_a = 1 - F_n/(a\sigma T_0^4)]$, it was necessary to assume a value for the surface emissivity a. The value of 0.90, found by Falckenburg (1928) for desert soils, was assumed here. The surface temperature T_0 was measured by means of a silicone insulated resistance thermometer lying on the ground. Vapor pressure was measured psychrometrically in the lowest 10 cm. On some occasions vapor pressure was not measured, but was available from the U. S. Weather Bureau station at Tucson International Airport, about a half mile away. The measurements are all for 2045 MST on clear or mostly clear nights. At this hour of the day the nocturnal inversion is not yet strongly established. On two occasions scattered clouds, which later dissipated, obviously contributed to ϵ_a. Therefore, these values of ϵ_a were repositioned downward on the basis of backward extrapolation from values of ϵ_a for times after the clouds dissipated.

The measured ϵ_a increases with e, but all points exceed the computed ϵ_a, for 1000 mb, the mean excess

being about 0.03. The excess over a curve for 910 mb (approximately the pressure at Tucson) would be slightly larger. In view of the fact that aerosol and unknown trace gas emitters have been of necessity omitted from the computations, the excess of measured over computed is to be expected and the agreement could be considered encouraging. However, several possible errors limit the significance of the comparison. Errors in the measured net radiation are usually estimated to be as large as 25% on the basis of intercomparison of various radiometers. An error of this size may introduce an error as large as 0.04 in ϵ_a, as could an error of a few hundredths in the ground emissivity. Departures of the actual temperature and dew-point soundings from linearity could also be significant. Surface temperature inversions occurred on none of the 1700 MST soundings but were invariably present the following morning at 0500. A plot of observed surface vapor pressure vs total precipitable water showed considerable scatter. The computed ϵ_a is subject to errors in the basic emissivities and errors in the technique of computation. It is beyond the scope of the present paper to discuss the errors in the emissivities, but the differences between various published H_2O emissivities suggest that significant uncertainties may still be present. The use of emissivities for homogeneous slabs also has potential for error, although the error should be relatively small for the computation of downward flux density at the surface, especially when effective slab pressures are obtained by weighting with optical depth. The assumption of a constant 0.05 contribution to ϵ_a by O_3 can, as noted above, easily be in error by ± 0.01. A similar error is possible for overlap. The contribution by CO_2 is probably least in error. In any event, the various sources of error in the computed ϵ_a *may* be additive and of sufficient magnitude to make up the difference between measured and computed ϵ_a, just as the errors in measured ϵ_a *may* be of sufficient magnitude to account for the differences.

There is scant independent evidence for significant aerosol radiation. Visibilities exceeded 30 mi at all times, suggesting very aerosol-free air. Further evidence that aerosol radiation is relatively small is provided by measurements of total aerosol, or Mie, optical depth at 0.4290 μ by Herman *et al.* (1971) at Tucson under weather conditions similar to those involved in the observations of Sellers and Dryden. The average was 0.07, which is substantially below the value 0.23 found at Los Angeles with "typical" haze conditions. Unfortunately, so little is known about aerosol radiation that one cannot say with certainty that its contribution is negligible.

The measurements are not inconsistent with the findings of Robinson (1950) that measured downward flux density exceeds the computed. If the difference found here is real, the most likely sources of radiation appear to be aerosols or unspecified trace gases.

8. Concluding remarks

The accuracy of the effective atmospheric emissivity is limited by the absence of a computation of the flux density contributed by aerosols (and possibly by unspecified trace gases), and by the use of laboratory emissivities for a homogeneous atmosphere. The aerosol contribution represents an unsolved problem which limits the applicability of flux computations by any method. The computation by means of emissivities for homogeneous slabs introduces errors that depend on various factors, especially the method of computation, but which are relatively small for the computation of downward flux density at the surface. Goody (1964) notes that various methods of flux computations lead to net fluxes and cooling rates that differ on the order of 50% from each other, but he cannot explain the differences. Rodgers and Walshaw (1966) add still another method of computation, claimed to be more accurate than existing techniques, but do not explain differences between previous results and their results.

Discrepancies between various methods of computation can probably best be understood by first resolving discrepancies in the computed downward flux density at the earth's surface for the simplest distributions of temperature and emitters, such as the straight line distributions used in this paper. To attempt to understand directly the discrepancies in net radiation and cooling rate in a typical, irregular sounding is unrealistic because the net radiation requires the difference of two flux densities, while the cooling rate requires the vertical gradient of the net radiation.

Acknowledgments. The research reported in this paper has been supported by the Office of Naval Research under Contract Nonr N 00014-67-A-0209-0004.

REFERENCES

Elsasser, W. M., 1942: Heat transfer by infrared radiation in the atmosphere. *Harvard Meteor. Studies*, No. 6, Cambridge, Harvard University Press, 107 pp.

——, with M. F. Culbertson, 1960: Atmospheric radiation tables. *Meteor. Monogr.*, 4, No. 23, 1–43.

Falckenberg, G., 1928: Die Absorptionskonstanten einiger meteorologisch wichtiger Korper für infrarote Wellen. *Meteor. Z.*, 45, 334–337.

Goody, R. M., 1964: *Atmospheric Radiation.* Oxford, Clarendon Press, 436 pp.

Haltiner, G. J., and F. L. Martin, 1957: *Dynamical and Physical Meteorology.* New York, McGraw-Hill, 470 pp.

Herman, B. M., S. R. Browning and R. J. Curran, 1971: The effect of atmospheric aerosols on scattered sunlight. *J. Atmos. Sci.*, 28, 419–428.

Junge, C. E., 1963: *Air Chemistry and Radioactivity.* New York, Academic Press, 382 pp.

Jurica, G. M., 1970: Radiative flux densities and heating rates in the atmosphere using pressure and temperature-dependent emissivities. Ph.D. dissertation, University of Arizona.

Kondrat'yev, K. Ya., 1965: *Radiative Heat Exchange in the Atmosphere.* London, Pergamon Press, 411 pp.

Kozyrev, B. P., and V. A. Bazhenov, 1969: Role of minor atmospheric constituents in infrared radiation absorption. *Izv. Atmos. Oceanic Phys.*, 5, 422–425.

Robinson, G. D., 1947: Note on the measurement and estimation of atmospheric radiation, 1. *Quart. J. Roy. Meteor. Soc.*, **73**, 127–150.

——, 1950: Note on the measurement and estimation of atmospheric radiation, 2. *Quart. J. Roy. Meteor. Soc.*, **76**, 37–51.

——, 1966: Some determinations of atmospheric absorption by measurement of solar radiation from aircraft and at the surface. *Quart. J. Roy. Meteor. Soc.*, **92**, 263–269.

Rodgers, C. D., 1967: The use of emissivity in atmospheric radiation calculations. *Quart. J. Roy. Meteor. Soc.*, **93**, 43–54.

——, and C. D. Walshaw, 1966: The computation of infrared cooling rate in planetary atmospheres. *Quart. J. Roy. Meteor. Soc.*, **92**, 67–92.

Sellers, W. D., and P. S. Dryden, 1967: An investigation of heat transfer from bare soil, Final Rept., Grant DA-AMC-28-043-66-G27, Institute of Atmospheric Physics, University of Arizona, Tucson.

Staley, D. O., and G. M. Jurica, 1970: Flux emissivity tables for water vapor, carbon dioxide and ozone. *J. Appl. Meteor.*, **9**, 365–372.

Swinbank, W. C., 1963: Long-wave radiation from clear skies. *Quart. J. Roy. Meteor. Soc.*, **89**, 339–348.

Wyatt, P. J., V. R. Stull and G. N. Plass, 1962: The infrared absorption of water vapor. Final Rept., SSD-TDR-62-127, Vol. II, Aeronautronic Div., Ford Motor Co., 249 pp.

Zdunkowski, W. G., R. E. Barth and F. A. Lombardo, 1966: Discussion of the atmospheric radiation tables by Elsasser and Culbertson. *Pure Appl. Geophys.*, **63**, 211–219.